ZERO-POWER MAGNETOMETERS WITH REMOTE OPTICAL INTERROGATION

Daniel J. Vasquez and Jack W. Judy

Electrical Engineering Department University of California, Los Angeles, USA
Email: dvasquez@ee.ucla.edu, jjudy@ee.ucla.edu

ABSTRACT

A magnetic-field-sensing system that consists of a miniature zero-power magnetometer, an integrated micromachined corner-cube reflector (CCR), commercially available diode laser, and a photo-detector array, has been designed, fabricated, assembled, and tested. The sensor node occupies a volume of only 1.5 mm^3 and can detect a magnetic field between 0 to 6 kA/m. The primary application of this technology is in wireless sensing systems that must operate continuously without providing or maintaining the sensor-node energy (e.g., replacing batteries or scavenging energy) or in extremely harsh environments.

1. INTRODUCTION

Networks of many small and low-power sensors can be used to monitor distributed data sets. Applications for such networks exist in the commercial, environmental, industrial, and military domains, and range from measuring seismic activity, ground-water contamination, security, and machine or equipment failure [1]. A sensor node typically consists of five components: sensor, processor, memory, power supply, and transceiver [1]. Because battery technology has not kept pace with hardware advances, the power supply of sensor networks, along with single-node cost, has become a major bottleneck in designing networks with the scale and density desired by many applications. It is important to note that since magnetometers are particularly power hungry, their use greatly limits the operational lifetime of magnetometer sensor networks. Consequentially, it is critical that the sensor node consume as little energy as possible. For some applications, low-power sensors and infrequent telemetry can achieve a sufficiently long node lifetime before the battery must be replaced or the node is discarded. However, for permanent sensor-network installations, the node must either scavenge energy from its environment, receive remotely directed power, or require no power at all.

Although sensor nodes have been developed that scavenges energy from the sun [2], vibrations [3-5], and walking (i.e., heel strike) [6], these strategies limit sensor-node distribution to energy-rich environments.

Remote powering is the ability to deliver power to an individual node from a remote source to eliminate the need for an on-board supply. Two approaches for remote powering include optical powering [7], where an external laser is used to power a node, and inductive powering [8-9], where an external drive coil is used to power an inductively coupled secondary coil. Inductive powering is a technology that has gained interest in the field of implantable devices [9]. However, inductive powering is only practical where the power supply is in close proximity to the sensor node.

In addition to power and cost limitations there are concerns about the durability of sensor nodes deployed in harsh or hostile locations. Applications with harsh environmental demands include those in the industrial, automotive, and aerospace domains where temperatures can exceed 200°C [7]. Temperatures this high can cause conventional integrated circuits (ICs) to fail [7].

In this paper, we describe a miniature sensor node that is capable of measuring magnetic fields and can be remotely interrogated at a considerable distance without ICs, a power supply, energy scavenging, or remote powering,

2. THEORY

MEMS Magnetometer

While existing magnetometers typically require substantial drive currents and are generally power hungry, recently, a ferromagnetic MEMS magnetometer has been developed that transduces the magnetic signal into a mechanical signal without any external power supply. However, in order to convert the mechanical signal into an electrical signal, low-power ICs are used, and ultimately limit the power consumption of the sensor [10-11].

The design and performance of the ferromagnetic MEMS magnetometer operates in a manner similar to a microcompass by translating magnetic fields into mechanical movement [10], and consists of a magnetic element attached to a pair of symmetric torsion beams (Fig. 1).

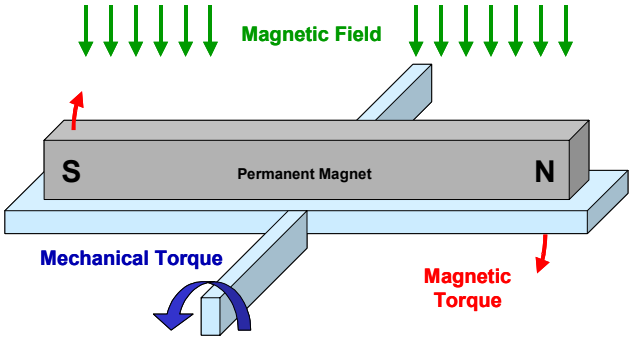

Figure 1: Schematic diagram of the ferromagnetic MEMS magnetometer.

In the presence of a magnetic field, the magnetic element will experience a magnetic torque, and like a compass, it will rotate to align its magnetization vector so that it is in the same direction as the magnetic field. However, unlike a compass, the rotation of the magnetic element is opposed by a mechanical torque applied from the torsion springs. By equating the magnetic and mechanical torques, the overall angle of deflection, ϕ_{mag}, can be expressed as

$$\phi_{mag} = \frac{(M \times H) \cdot V_{mag}}{k_\phi} \quad , \qquad (1)$$

where M is the magnetization of the magnetic element, H is the magnetic field, V_{mag} is the volume of the magnetic element, and k_ϕ is the torsional spring constant [10]. Although the mechanical deflection of the magnetic element only requires the presence of a magnetic field and does not require any input power, power is still required by the sensing circuitry to convert the mechanical movement into an electrical value. In addition, if used in a typical sensor node, power will also be required for radio transmission.

Corner-Cube Reflector (CCR)

An ideal CCR consists of three mutually orthogonal mirrors as shown in Figure 2.

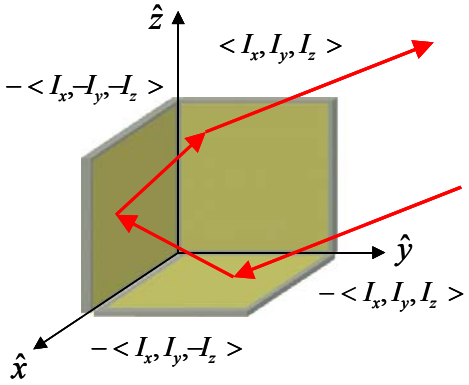

Figure 2: Ideal CCR and defined coordinate system.

When light from a source reflects off of all three mirrors, it is directed back towards the light source regardless of the incident direction (Fig. 3a). However, when one of the three mirrors in a CCR is misaligned, two distinct reflected beams emerge from the corner cube (Fig. 3b).

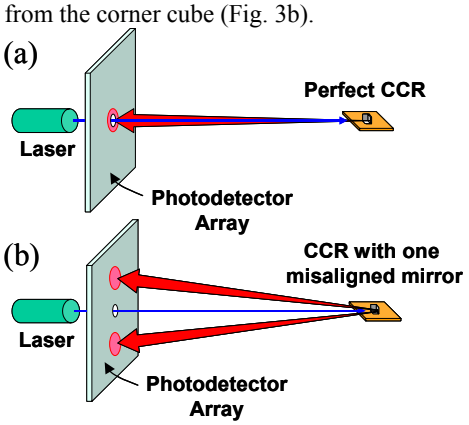

Figure 3: A CCR will reflect light (a) towards the source when aligned and (b) split into two beams when one mirror is misaligned.

The full angle of divergence of the two optical beams is a function of the incident direction and the amount of misalignment of the non-ideal mirror. By digitally modulating one of the three mirrors, it is possible to use a CCR for digital optical communications [2,12-13].

By ray tracing through a CCR, the reflected direction of the optical beams can be found. Because there are six distinct paths through a CCR, there is the potential for six different reflected directions. However, if only a single mirror is misaligned and the other two mirrors remain orthogonal to each other, only two of the reflected directions are unique. If the two reflected directions R_1, and R_2, are each normalized, the cosine of the angle between the reflected optical beams is equal to their dot product. Assuming the coordinate system illustrated in Fig. 2, the dot product R_1 and R_2 can defined as

$$R_1 \bullet R_2 = I_x{}^2 + (I_y{}^2 + I_z{}^2) \cdot \cos(4 \cdot \phi_{mirror}) \quad , \qquad (2)$$

where ϕ_{mirror} is the angle of misalignment of the non-ideal mirror, and I is the normalized incident direction. Using the small-angle approximation, we can find that the angle between R_1 and R_2 is given by

$$\theta_{R_1 R_2} \approx 4 \cdot (I_y{}^2 + I_z{}^2) \cdot \phi_{mirror} \quad . \qquad (3)$$

3. Design

By coupling the rotation of the movable mirror to the rotation of the magnetic sensor, it is possible to create a magnetometer that does not require or consume any power at the remote location. In our design, the magnetometers consist of magnetic elements that are torsionally suspended at one end to allow for a greater degree of rotation. A pair of magnetometers is integrated with a CCR so that the misalignment of one mirror of the CCR is directly coupled to the angular deflection of the magnetometers, as shown in Figure 4. The angular movement of the magnetometer is dependent on the size of the magnetic elements, their magnetization, the strength of the ambient magnetic field, and the stiffness of the supporting torsion beam [4-5].

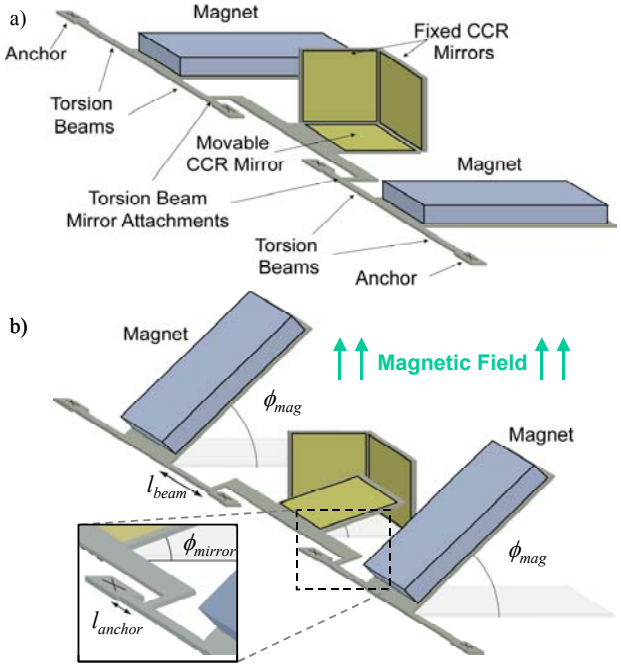

Figure 4: Zero-power sensor (a) without (b) with magnetic field applied.

In the current design, the movable mirror is attached near the anchors of the torsion beams that suspend the magnetic elements (Fig. 4). This was done to facilitate testing, since it would scale down the larger angle of magnetic-element rotation to a much smaller and more manageable mirror angle of rotation. The angle of mirror misalignment is given by

$$\phi_{mirror} = \phi_{mag} \frac{l_{anchor}}{l_{beam}} \quad , \tag{4}$$

where l_{anchor} is the length between the torsion-beam anchor and the position on the torsion beam where the mirror is attached, and l_{beam} is the length of the torsion beam. The sensitivity of the device can be increased by connecting the mirror directly to the magnetic element.

Dependence on Orientation

By ray-tracing through the corner cube, it is noted that the angle between the two reflected optical beams is a function of both mirror misalignment as well as the incident direction of the incoming laser. The dependence on incident direction is a non-ideality in terms of sensor performance if the orientation of the CCR is not known. For these cases we propose to have a calibration CCR fabricated with a known ϕ_{mirror} mounted next to the CCR sensor. Each of the two different CCRs need to be packaged in its own filtered enclosure so that their signals can be distinguished. Under this scenario, the sensor-mirror-misalignment angle can be found from the ratio of $\theta_{R_1R_2-sensor}$ and $\theta_{R_1R_2-known}$ for the sensor and the calibration CCR respectively, where we find that:

$$\phi_{mirror-sensor} = \frac{\theta_{R_1R_2-sensor}}{\theta_{R_1R_2-known}} \cdot \phi_{mirror-known} \quad . \tag{5}$$

4. Fabrication

The zero-power magnetometers were fabricated using the Multi-Users MEMS Processes (MUMPs) [14], which is a standard surface-micromachining foundry process. The MUMPs process consists of a 2-µm thick and a 1.5-µm thick polysilicon structural layer, two sacrificial oxides, and a gold layer. While the MUMPs process provided enough structural layers for the design of the CCRs, it does not contain any ferromagnetic layers. An extra layer of CoNi was electroplated onto the chips in a post-processing step. The final gold layer of the MUMPs process was used as the seed layer for the electrodeposition. First a 100-nm-thick Ti layer was deposited across the entire chip using an e-beam evaporator (CHA mark 40). Next the plating mold is defined using photolithography with Shipley SJR5640 positive photoresist. The exposed Ti conduction layer is then removed over the seed layer in a 1:100 HF solution. Finally, CoNi was electroplated onto the gold seed layer, the photoresist was stripped (Fig. 5a), the entire structure was released in 49% HF for 4 minutes, and then the CCRs were carefully assembled (Fig. 5b).

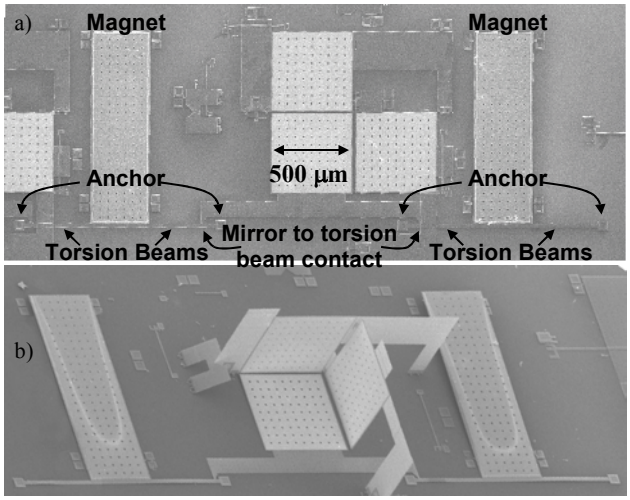

Figure 5: SEM of an (a) unassembled zero-power sensor and (b) assembled zero-power sensor.

5. Experimental Setup And Results

To test the sensor system, the CCR magnetometer is mounted onto a magnetic coil and the pair of optical beams reflected back by the CCR are projected onto a screen and captured by a photodetector array. The screen and photodetector array were located 1 m away from the magnetometer/CCR. A sample image reflected back from the zero-power sensor node is given in Figure 6, with the theoretically calculated beam position indicated. The roughness, curvature, and small size of the surface-micromachined mirrors causes a larger and diffuse beam spot, the beam spot could be improved by using slightly larger, smoother, and flatter mirrors (e.g., bulk-micromachined mirrors).

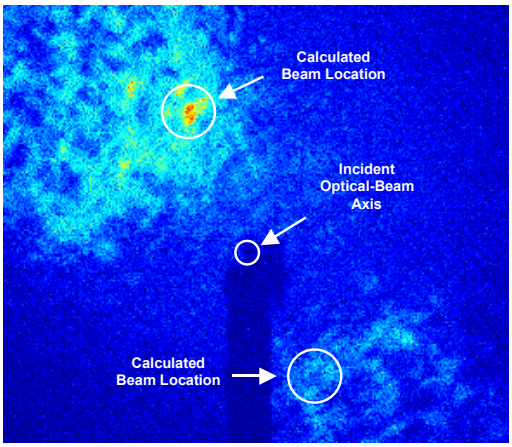

Figure 6: Image of the pair of optical beams reflected from the zero-power magnetometer.

The experimental results were obtained with a CCR that had 500-µm wide mirrors, with a 3-cm radius of curvature. The measured results agree well with the theoretical calculations (Fig. 7 and 8).

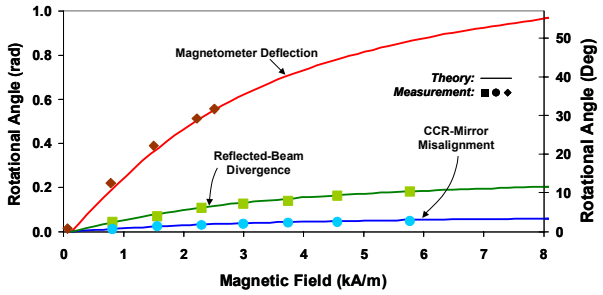

Figure 7: Theoretical and measured data for magnetic element deflection, CCR-mirror misalignment, and reflected-beam divergence.

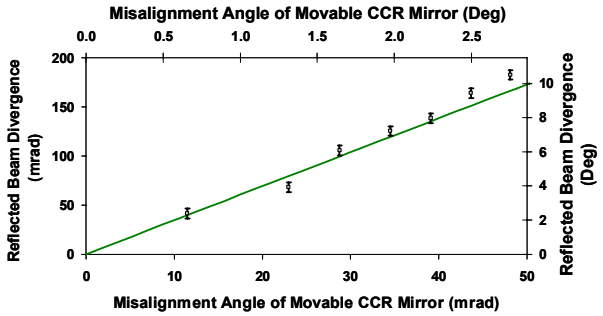

Figure 8: Plot of reflected beam divergence vs. mirror misalignment.

The ultimate detection range is intimately tied to the magnetometer design, desired dynamic range, and mirror size/quality. Theoretical calculations indicate that a diffraction and noise limited analog response from 1-mm-diameter mirrors is possible at 100 m.

6. Conclusion

It is possible to create zero-power magnetometers that can be optically interrogated by a remote laser and photo-detector array. A micromachined CCR and ferromagnetic MEMS magnetometer have been integrated and used to detect magnetic fields varying from 0 to 6 kA/m at an optical interrogation range of 1 m. The use of CCRs in analog modulation mode enables a simplified node architecture by eliminating the need for sensing circuitry, power supplies, and radio equipment, thus reducing the size and cost of a sensor node tremendously. The first-generation prototype zero-power magnetometers only required a volume of ~1.5 mm^3. It is expected that subsequent sensor nodes will be even smaller. Theoretically analog CCRs have the capability of operating in the 100-m range, but are limited by mirror curvature, roughness, and diffraction. More work can be done to improve sensor performance by reducing mirror curvature, increasing mirror size through bulk-fabricated mirrors [13], and increasing sensor sensitivity by increasing the magnetic volume and attaching the mirrors directly to the magnetic elements.

7. Acknowledgements

The authors would like to thank Jeff Yee for his help with the magnetometer design, Lixia Zhou and Kris Pister for supplying us with their MUMPs digital CCR layout from which we based our CCR layout, and Bongyoung Yoo for electroplating our magnetic sensors. The authors also acknowledge The Eugene Cota Robles Fellowship, DARPA DABT63-99-1-0020, and NSF Career Award ECS9876285 for their financial support.

8. References

[1] M. Tubaishat and S. Madria, "Sensor networks: an overview," *IEEE Potentials, Vol*, vol. 22, no. 2, pp. 20-23, April-May 2003.

[2] B.A. Warneke, M.D. Scott, B.S. Leibowitz, Z. Lixia, C.L. Bellew, J.A. Chediak, J.M. Kahn, B.E. Boser, and K.S.J. Pister, "An autonomous 16 mm^3 solar-powered node for distributed wireless sensor networks," *Proceedings of IEEE Sensors 2002, 1st IEEE International Conference on Sensors*, 2002.

[3] S. Roundy, P.K. Wright, and K.S.J. Pister, "Micro-Electrostatic Vibration-to-Electricity Converters," *Proceedings of ASME International Mechanical Engineering Congress & Exposition (IMECE2002)*, November, 17-22, 2002.

[4] S. Meninger, J.O. Mur-Miranda, R. Amirtharajah, A. Chandrakasan, and J.H. Lang, "Vibration-to-electric energy conversion," *IEEE Transactions on VLSI Systems,* vol. 9, no. 1, pp. 64-76, Feb. 2001.

[5] C.B. Williams and R.B. Yates, "Analysis of a micro-electric generator for microsystems," *Sensors and Actuators A (Physical)*, vol. A52, no. 1-3, pp. 8-11, 1996.

[6] N.S. Shenck and J.A. Paradiso, "Energy scavenging with shoe-mounted piezoelectrics," *IEEE Micro*, vol. 21, no. 3, pp. 30-42, 2001.

[7] M. Suster, W.H. Ko, and D.J. Young, "Optically-Powered Wireless Transmitter for High-Temperature MEMS Sensing and Communication," *International Conference on Solid-State Sensor and Actuators (Transducers 2003)*, Boston, USA, (June 8-12, 2003) pp. 1073-1076.

[8] S. Takeuchi and I. Shimoyama, "Selective drive of electrostatic actuators using remote inductive powering," *Sensors and Actuators A (Physical)*, vol. 95, no. 2-3, pp. 269-273, 2002.

[9] K. Van Schuylenbergh and R. Puers, "Self-tuning inductive powering for implantable telemetric monitoring systems," *Sensors and Actuators A-Physical*, vol. A52, no. 1-3, pp. 1-7, 1996.

[10] J.K. Yee, H.H. Yang, and J.W. Judy, "Shock resistance of ferromagnetic micromechanical magnetometers," *Sensors & Actuators A-Physical,* vol. A103, no. 1-2, pp. 242-252, Jan, 2003.

[11] H.H. Yang, N.V. Myung, J. Yee, D.-Y. Park, B.-Y. Yob, M. Schwartz, K. Nobe, and J.W. Judy, "Ferromagnetic micromechanical magnetometer," *Sensors and Actuators A (Physical)*, vol. A97-A98, pp. 88-97, 2002.

[12] Z. Lixia, J.M. Kahn, and K.S.J. Pister, "Corner-cube retroreflectors based on structure-assisted assembly for free-space optical communication," *Journal of Microelectromechanical Systems,* vol. 12, no. 3, pp. 233-242, June, 2003.

[13] Z. Lixia, K.S.J. Pister, and J.M. Kahn, "Assembled corner-cube retroreflector quadruplet," *IEEE Micro Electro Mechanical Systems Workshop (MEMS 2002)*, Las Vegas, Nevada, (January 20-24, 2002).

[14] MEMSCAP, *http://www.memscap.com/memsrus/crmumps.html*